JOURNAL OF WATER AND LAND DEVELOPMENT
e-ISSN 2083-4535
Polish Academy of Sciences (PAN) Institute of Technology and Life Sciences – National Research Institute (ITP – PIB)

JOURNAL OF WATER AND LAND DEVELOPMENT
DOI: 10.24425/jwld.2026.157838
2026, No. 68 (I–III): 224–235

Stage temperature boosting in solar membrane distillation systems for agricultural wastewater treatment using waste heat recovery

Otabek Mukhitdinov*[1)], Doniyor Jumanazarov[2)], Egambergan Khudoynazarov[3)], Elyor Saitov[4)]

[1)] Kimyo International University in Tashkent, Mechanical Engineering, 156 Shota Rustaveli St, Tashkent, 100121, Uzbekistan
[2)] Urgench State University, Department of Physics, 14 Kh. Alimdjan St, 220100, Urgench, Uzbekistan
[3)] Mamun University, 2 Bolkhovuz St, Khiva, 220900, Uzbekistan
[4)] University of Tashkent for Applied Sciences, Department of Materials Science, 1 Gavkhar St, Tashkent, 100149, Uzbekistan

* Corresponding author

RECEIVED 05.09.2025 ACCEPTED 26.11.2025 AVAILABLE ONLINE 31.03.2026

Abstract: Solar-powered membrane distillation for agricultural wastewater is limited by temperature polarisation and solar intermittency. This study evaluates stage temperature boosting – injecting low-grade agricultural waste heat at intermediate stages – in an eight-stage air-gap membrane distillation (AGMD) pilot operated at an agricultural research facility in the Fergana Valley (Uzbekistan). Under high irradiance (>800 $W \cdot m^{-2}$), distillate flux increased by 88% from 6.5 ±0.4 to 12.2 ±0.6 $kg \cdot m^{-2} \cdot h^{-1}$ ($n = 3$, $p < 0.001$), and under low irradiance (<500 $W \cdot m^{-2}$) from 2.8 ±0.3 to 9.1 ±0.5 $kg \cdot m^{-2} \cdot h^{-1}$ ($n = 3$, $p < 0.001$). Uptime (flux ≥80% of nominal) improved from 67 to 92%. Energy efficiency rose markedly: gained output ratio (*GOR*) increased by 161% from 3.1 ±0.3 to 8.1 ±0.5 ($p < 0.001$). Total specific energy consumption decreased by 62% to 145.0 ±11.4 $kWh \cdot m^{-3}$, driven by lower thermal demand (specific thermal energy consumption, SEC_{th}: from 375 ±28 to 138 ±11 $kWh \cdot m^{-3}$) with a modest electrical increase (specific electrical energy consumption, SEC_{el}: from 2.8 ±0.2 to 7.0 ±0.4 $kWh \cdot m^{-3}$). Permeate quality remained high (total dissolved solids (*TDS*) rejection >99.5%; *Escherichia coli* not detected). By sustaining the thermal driving force and mitigating polarisation, stage temperature boosting couples solar input with site-available waste heat to deliver robust, energy-efficient water reclamation for agriculture.

Keywords: agricultural wastewater, membrane distillation, solar energy, stage temperature boosting, waste heat recovery

INTRODUCTION

Rising global demand for freshwater, driven by population growth and rapid industrialisation, is putting water security at risk, especially in arid and semiarid regions (Jain *et al.*, 2024). Agriculture uses the most freshwater, a pattern seen in countries such as Uzbekistan (Turaeva and Sultanova, 2024). Heavy reliance on nonrenewable groundwater intensifies pressure on scarce supplies and threatens the long-term sustainability of farm productivity (Karimov *et al.*, 2022). Sustainable water management is therefore essential for food security and environmental protection (Chathuranika *et al.*, 2022). In line with Uzbekistan's priorities for water security and agricultural growth, there is an urgent need for technologies that raise water use efficiency and expand the use of nonconventional water sources for irrigation (Hamidov *et al.*, 2024; Bobocholov, Hamidov and Bellingrath-Kimura, 2025). Treating agricultural wastewater, including irrigation return flows, for reuse offers a practical route toward a circular economy in agriculture, easing water scarcity while lowering the environmental burden of agricultural discharge (Fito and Hulle van, 2021; Mannina, Gulhan and Ni, 2022; Christou *et al.*, 2024).

Membrane technologies are effective for many wastewater treatment tasks because they are efficient, modular, and have a small footprint (Bera, Godhaniya and Kothari, 2022; Foorginezhad *et al.*, 2025). Within this group, membrane distillation is a thermal separation method with clear advantages for streams with high salinity or complex contaminants, including those from agriculture (Ibrahim *et al.*, 2023; Ngo *et al.*, 2023; Natesan and Purushothaman, 2025). In contrast with pressure-driven options such as reverse osmosis, membrane distillation works at low hydraulic pressure, which lowers the risk of membrane fouling (Singh *et al.*, 2023). It can run on low-grade or waste heat, which supports coupling with renewable energy sources and advances sustainability goals (Sarbu, Mirza and Muntean, 2022; Ji *et al.*, 2024).

Solar energy is abundant and clean. Pairing it with solar-powered membrane distillation is a major focus for sustainable desalination and water treatment (AlMallahi *et al.*, 2024; Jawed *et al.*, 2024). In solar-powered membrane distillation, solar thermal energy creates the temperature difference across a hydrophobic microporous membrane. This drives water vapour through the membrane while blocking nonvolatile contaminants (Maqbool *et al.*, 2025). The method can remove salts, heavy metals, and organic compounds at high rejection rates and yields a distillate suitable for agricultural reuse (Egbuikwem *et al.*, 2021).

Even with these advantages, conventional solar-powered membrane distillation faces several built-in obstacles. A key issue is temperature polarisation (Jawed *et al.*, 2024). Temperature polarisation is the drop in the temperature difference at the membrane feed interface relative to the bulk feed. It arises from heat loss during evaporation and from heat conduction through the membrane (Hijaz *et al.*, 2023). The smaller temperature difference lowers the vapour pressure driving force for membrane distillation, which cuts permeate flux and reduces overall thermal efficiency (Son *et al.*, 2021). System output also depends on daily and seasonal swings in solar irradiance, which leads to intermittent operation and lower productivity during periods with weak sunlight (Vasisht, Srinivasan and Ramasesha, 2016).

Researchers have used several methods to boost the performance and energy efficiency of membrane distillation systems. Multistage setups recycle latent heat released during condensation to preheat downstream feed and thus raise the gained output ratio (*GOR*), defined as the ratio of latent heat embodied in produced distillate to total external heat input, a central measure of thermal efficiency (Liu *et al.*, 2023; Al Hariri and Khalifa, 2025). Different layouts have been tested. Air gap membrane distillation (AGMD) aims to reduce conductive heat losses and improve thermal efficiency (Francis, Ahmed and Hilal, 2022; Gopi *et al.*, 2023). It places a still layer of air between the membrane and the condenser surface, which serves as insulation (Kalenik *et al.*, 2023; Wałowski, 2023). The tradeoff is extra resistance to mass transfer, which can lower permeate flux when compared with direct contact membrane distillation (DCMD) (Escorcia *et al.*, 2025). Recent work has focused on better module design, new membranes with stronger photothermal response, and hybrid systems to address these limits (Chang *et al.*, 2022).

Although multistage and solar-integrated designs show promise, a major and underexplored opportunity is to use low-grade waste heat already available in agricultural operations (Sebo *et al.*, 2025). Greenhouses, livestock housing, and anaerobic digesters produce large amounts of low-temperature waste heat that usually escapes to the environment (Mengqi *et al.*, 2023). Capturing and using this heat can provide a steady supplemental energy source to support solar thermal input, which in turn addresses key limits of conventional solar-powered membrane distillation systems (Hasan *et al.*, 2023).

Most prior work has targeted better solar collection or improved internal heat recovery within the membrane distillation unit itself (Huang *et al.*, 2023). A systematic study of raising stage temperatures from outside the multistage solar membrane distillation system with agricultural waste heat is missing. This gap matters. If low-grade heat is injected at well-chosen points in a multistage layout, the system can counter temperature polarisation, keep a strong thermal gradient across stages, and reduce dependence on variable solar radiation. Such a strategy can reshape the energy balance of membrane distillation and yield a more robust, efficient, and cost-effective approach to treating agricultural wastewater.

Prior demonstrations of solar-integrated membrane distillation have largely (i) intensified internal heat recovery to raise latent-heat reuse or (ii) improved solar capture and storage; both paths remain sensitive to cumulative temperature decay along multistage trains and to irradiance variability. External waste-heat coupling has been discussed conceptually for agriculture, but explicit mid-stage thermal injection in multistage AGMD has not been evaluated at pilot scale. This study advances the state of knowledge by externally restoring the stage-wise thermal gradient at targeted nodes using low-grade, site-available heat, thereby directly weakening temperature polarisation, stabilising flux under low irradiance, and shifting the energy balance toward a higher *GOR* without compromising permeate quality.

This study sets itself apart from prior work by proposing and testing a new stage temperature boosting framework. Rather than focusing only on solar energy or only on internal heat recovery, it examines how solar thermal energy can work together with heat recovered from agricultural waste in a multistage AGMD system tailored to treat contaminated irrigation return flows.

The motivation is the urgent need for water treatment that is both energy efficient and reliable for agriculture. The stage temperature boosting approach fits this need because it targets the main performance limits of solar-powered membrane distillation, namely temperature polarisation and solar intermittency, by drawing on an underused onsite energy resource (Zewdie *et al.*, 2021). A multistage AGMD configuration was selected for its potential to deliver high thermal efficiency and for its robustness with high salinity feeds that typify irrigation return flows (Heeley *et al.*, 2024).

The main aim of this research is to investigate the performance of a novel multi-stage solar membrane distillation system enhanced by stage temperature boosting using agricultural waste heat for the treatment of contaminated irrigation return flows.

The specific objectives of this study are:

- to design and construct a pilot-scale, eight-stage AGMD system with integrated waste heat injection points for strategic temperature boosting;
- to evaluate the system's performance in terms of distillate flux, contaminant removal efficiency, and energy utilisation under varying solar radiation and waste heat availability scenarios,

using irrigation return flows from agricultural sites in the Fergana Valley region of Uzbekistan;
- to conduct advanced thermal modelling to elucidate the vapour transport mechanisms and the impact of temperature boosting on mitigating temperature polarisation effects;
- to assess the overall improvement in system uptime, specific energy consumption, and water quality compared to a conventional solar-only membrane distillation system.

Hypotheses. We test five pre-specified hypotheses: (H1) stage temperature boosting increases time-averaged flux relative to a solar-only baseline, (H2) boosting increases *GOR* and lowers total specific electrical energy consumption (SEC_{el}) by reducing thermal demand, (H3) boosting increases uptime under low irradiance, (H4) boosting maintains contaminant rejection comparable to the baseline, and (H5) boosting increases the temperature polarisation coefficient (*TPC*) by elevating feed-side membrane surface temperature.

This study offers three main contributions to membrane distillation. First, it introduces and validates stage temperature boosting as a new approach for designing energy-efficient systems. Second, it presents the first comprehensive experiments on coupling diverse agricultural waste heat sources with a multi-stage solar membrane distillation platform. These results provide new insight into reducing temperature polarisation and improving the operational resilience of solar-powered membrane distillation. Finally, the work demonstrates a robust, decentralised water treatment technology that turns agricultural wastewater into a valuable resource, supports sustainable farming and circular economy goals, and strengthens water security in arid regions.

MATERIALS AND METHODS

EXPERIMENTAL SITE AND WASTEWATER CHARACTERISATION

This study took place at a dedicated agricultural research facility in the Fergana Valley in eastern Uzbekistan. The site was chosen because it represents a continental arid climate and hosts diverse farming operations, which provide access to the target wastewater stream and to relevant waste heat sources.

The membrane distillation feedwater came from irrigation return flows collected at a commercial cotton farm. This wastewater is typical of field drainage in the region and contains elevated salts, fertilisers, and residual organic matter. Before each experimental run, we collected a 1000 dm^3 composite sample of the return flow and stored it in an opaque sealed tank to limit algal growth and changes in composition. At the start of the study, we completed a comprehensive characterisation to set a baseline for evaluating treatment performance. Key water quality parameters were analysed in triplicate, and average values are reported.

Total dissolved solids (*TDS*) and electrical conductivity (*EC*) were measured with a calibrated benchtop multiparameter meter Orion Versa Star Pro Thermo Fisher Scientific USA. The pH was measured with a calibrated pH electrode. Turbidity was measured with a nephelometric turbidimeter Hach 2100Q USA. Concentrations of major anions, including nitrates NO_3^- and phosphates PO_4^{3-}, were quantified by ion chromatography Dionex ICS 6000 Thermo Fisher Scientific USA following American Public Health Association (APHA) Standard Method 4110 B (APHA, AWWA, WEF, 2017). Total organic carbon (*TOC*) was analysed using a high temperature combustion *TOC* analyser Shimadzu TOC L Japan as described in APHA Standard Method 5310 B (APHA, AWWA, WEF, 2017). Microbiological contamination, specifically *Escherichia coli*, was assessed with the membrane filtration technique as defined in APHA Standard Method 9222 B (APHA, AWWA, WEF, 2017).

PILOT-SCALE MULTI-STAGE MEMBRANE DISTILLATION SYSTEM DESIGN AND FABRICATION

A pilot-scale experimental system was designed and built to test the stage temperature boosting concept. The system had three main parts, which were a solar thermal collector array, a multi-stage air gap membrane distillation (AGMD) module, and a waste heat recovery and injection loop.

An array of evacuated tube solar collectors with a total aperture area of 20 m^2 supplied the primary thermal energy. The collectors faced south at a fixed tilt of 40°, selected for year-round solar harvesting at the study latitude. A closed-loop circuit with a heat transfer fluid, a 50/50 mixture of propylene glycol and deionised water, transferred the captured heat to the feedwater through a 316 dm^3 stainless steel plate and frame heat exchanger. A variable speed centrifugal pump set the heat transfer fluid flow rate, which allowed control of the temperature of the feedwater entering the first stage of the membrane distillation module.

The core of the treatment system was an eight-stage AGMD module that was custom-fabricated from polypropylene to provide chemical resistance and thermal insulation. Each stage had an effective membrane area of 1.5 m^2, giving a total membrane area of 12 m^2. The stages were arranged vertically so that gravity assisted the flow of the feed and distillate streams.

Design rationale and operational stability. An eight-stage train balances internal heat recovery (via condenser-to-feed coupling) against hydraulic loss and module height, while providing sufficient downstream leverage for thermal "refresh" at multiple locations. Preliminary thermal screening identified stages 3, 5, and 7 as the steepest gradient-decay points; these were therefore selected for injection to re-establish the driving force. Flow and temperature control were held within instrument accuracy during all runs (thermocouples ±0.5°C; electromagnetic flow meters ±0.5%), and liquid entry pressure (*LEP* > 250 kPa for polyvinylidene fluoride (PVDF) membranes) was confirmed prior to each campaign, preventing wetting under the applied hydraulic conditions.

All stages used flat sheet hydrophobic PVDF membranes Durapore®, Merck Millipore, Germany. The membranes had a nominal pore size of 0.22 µm, a porosity of 75%, and a thickness of 125 µm. The *LEP*, verified with a dead-end filtration cell, was greater than 250 kPa, which prevented liquid water breakthrough under the operating pressures used.

Within each stage, the feed channel measured 1.5 m in length, 1.0 m in width, and 3 mm in depth. A 4 mm air gap separated the permeate side of the membrane from the condensation plate. The condensation plate in each stage also served as the preheating surface for the feed stream of the next stage, enabling internal heat recovery. The distillate was collected in a channel at the bottom of each condensation plate.

A waste heat recovery and injection system was built to simulate and use low-grade thermal energy from common agricultural sources. Based on earlier characterisation at the facility, we simulated three sources. The first was hot air from greenhouse cooling exhausts with temperatures of 50–60°C. The second was warm air from the livestock facility ventilation, with temperatures of 35–45°C. The third was heat from the cooling jacket of an anaerobic digester with temperatures of 65–75°C.

We captured the waste heat with liquid-coupled heat exchangers. Air-to-water units served the ventilation sources, and a water-to-water unit served the digester. The recovered heat was combined in one thermostatically controlled water loop. This loop fed compact plate and frame heat exchangers installed in the feed line at the inlet of stages 3, 5, and 7 of the AGMD module. These stages were selected as temperature boosting points because preliminary modelling showed the steepest decline in the temperature gradient there. A proportional–integral–derivative (PID) control system used temperature sensor inputs to adjust hot water flow through the boosting exchangers and hold the feed temperature setpoints at these intermediate stages.

The three simulated sources – greenhouse exhaust (50–60°C), livestock-barn ventilation (35–45°C), and anaerobic digester jackets (65–75°C) – reflect routinely observed temperature bands at the research site and in published operating ranges for comparable facilities. Combining sources into a single hydronic loop emulates practical retrofits in which low-grade heat is harvested opportunistically and mixed to supply stable mid-stage setpoints. The PID controller compensated source variability by modulating booster-loop flow to maintain stage-inlet targets (stages 3, 5, 7), ensuring that the imposed thermal profile brackets real agricultural duty cycles while isolating the effect of mid-stage injection on polarisation.

EXPERIMENTAL PROTOCOL AND OPERATING CONDITIONS

The system's performance was evaluated under two distinct operational modes over a period of six months, encompassing varying seasonal conditions. Each experimental run was conducted for eight continuous hours during daylight (08:00–16:00). A detailed run log with calendar dates, ambient temperature and wind speed at start/mid/end of each run, and daily irradiance summaries is provided in Table S1.

BASELINE OPERATION (SOLAR-ONLY)

In this control mode, we switched off the waste heat injection system. The plant then operated as a conventional multistage solar-powered membrane distillation system. The solar thermal collector array alone heated the feedwater to an inlet temperature of 80 ±2°C at the first stage. The feed flow rate was held at 300 $dm^3 \cdot h^{-1}$. Cooling water drawn from the feedwater at ambient temperature circulated through the final condenser at 400 $dm^3 \cdot h^{-1}$. We used this mode as the benchmark for evaluating the enhanced system.

STAGE TEMPERATURE BOOSTING OPERATION

Under this experimental mode, the stage temperature boosting system operated as designed. Primary solar heating raised the first-stage inlet to 80 ±2°C. The proportional–integral–derivative (PID) control system then used recovered waste heat to raise the feed temperature at the inlets of stages 3, 5, and 7 to at least 65°C. All other operating parameters, including feed flow rate and cooling water flow rate, matched the baseline to enable a direct comparison. Experiments were ran under high solar irradiance above 800 $W \cdot m^{-2}$ and under low irradiance below 500 $W \cdot m^{-2}$ to evaluate resilience to solar intermittency.

INSTRUMENTATION AND DATA ACQUISITION

The pilot plant was fully instrumented to monitor and record critical operating conditions. T–type thermocouples with ±0.5°C accuracy were placed at the inlet and outlet of every stage in the feed and coolant channels to map the temperature profile across the module. Electromagnetic flow meters with ±0.5% accuracy measured flow rates in the feed, coolant, and waste heat loops. Digital pressure transducers recorded pressure at the module inlet and outlet. A Kipp & Zonen CMP6 pyranometer mounted in the plane of the solar collectors measured incident solar irradiance. A centralised data acquisition system, National Instruments cRIO, logged all sensor readings at one-minute intervals. The cumulative mass of the distillate was tracked continuously with a digital balance with ±10 g accuracy connected to the logger.

Calibration and verification. Thermocouples were two-point calibrated (ice-bath and boiling-water references) at the start of each week; offsets were applied in the logger. Electromagnetic flow meters were verified monthly by timed volumetric drawdown over a calibrated vessel. Pressure transducers were zeroed to atmosphere before each run and checked against a dead-weight tester quarterly. The CMP6 pyranometer's factory calibration (World Meteorological Organization (WMO) traceable) was used; a cosine-response check was performed *in situ* by tilting relative to normal incidence.

ANALYTICAL PROCEDURES FOR WATER QUALITY ASSESSMENT

Samples of the feed, brine, and composite distillate were collected every two hours during each experimental run. The collected samples were analysed for the same set of parameters (total dissolved solids (*TDS*), electrical conductivity (*EC*), pH, turbidity, nitrates, phosphates, total organic carbon (*TOC*), and *E. coli*) using the identical standard methods and instrumentation. This allowed for a time-resolved assessment of the system's contaminant removal efficiency.

THERMAL MODELING AND PERFORMANCE METRICS

We developed a 2D computational fluid dynamics (CFD) model in ANSYS Fluent 2022 R1 to examine heat and mass transfer in the air gap membrane distillation (AGMD) module. The model represented a single AGMD stage with the feed channel, porous membrane, air gap, and condensation plate. It solved the coupled Navier–Stokes equations for fluid flow along with the energy and species transport equations. The membrane was treated as a porous medium, and evaporation and condensation at the interfaces followed the kinetic theory of gases. We used the model to visualise temperature and water vapour concentration profiles across the air gap and to evaluate how much the stage temperature boosting strategy reduced temperature polarisation.

Model specification and validation. Inlet boundary conditions imposed measured bulk feed temperature and a uniform velocity corresponding to the experimental per-stage flow; with a 3 mm feed-channel depth and 1 m width, the estimated Reynolds number is ≈170 (laminar). The outlet used fixed pressure; all walls were no-slip with conjugate conduction across solids. Evaporation at the feed interface used a kinetic (Hertz–Knudsen) expression, with saturation vapour pressure evaluated at the local membrane-surface temperature; the condenser surface was coupled to a convective sink matching measured coolant conditions. The membrane was a porous layer with effective thermal conductivity and permeability tuned to manufacturer specifications. A structured mesh with near-wall refinement resolved thermal and concentration boundary layers; mesh-independence gave <1% variation in stage-wise temperature polarisation coefficient (*TPC*). Validation compared simulated temperature profiles and TPC at a mid-module location to measurements, reproducing the observed increase from 0.91 (baseline) to 0.95 (boosted), consistent with the flux gains.

The experimental data were used to calculate several standard key performance indicators (KPIs) to quantify and compare the system's performance. The transmembrane distillate flux, J (kg·m^{-2}·h^{-1}), was calculated using Equation (1) (Hamidov *et al.*, 2024):

$$J = \frac{m}{A \cdot t} \tag{1}$$

where: m = the mass of the collected distillate (kg), A = the total membrane area (m^2), t = the operation time (h).

This fundamental metric indicates the productivity of the system per unit of membrane area. The contaminant rejection efficiency, R (%), was determined for various contaminants using Equation (2) (Sarbu, Mirza and Muntean, 2022):

$$R = \left(1 - \frac{C_p}{C_f}\right) \cdot 100 \tag{2}$$

where: C_p and C_f = the contaminant concentrations in the permeate (distillate) and feed streams, respectively.

This KPI is critical for evaluating the quality of the treated water and the effectiveness of the separation process. The thermal efficiency of the system was evaluated using the gained output ratio (*GOR*), a dimensionless metric calculated as shown in Equation (3) (Fito and Hulle van, 2021):

$$GOR = \frac{\sum (J_i \cdot A_i) \cdot H_v}{Q_{\text{in}}} \tag{3}$$

where: J_i and A_i = the flux and area of stage i, respectively, H_v = the latent heat of vaporisation of water (kJ·kg^{-1}), Q_{in} = the total rate of heat energy supplied to the system from both the solar collectors and the waste heat injection (kW).

The *GOR* represents the ratio of the energy required for evaporation to the total energy input, providing a measure of how effectively the system recovers and reuses latent heat. The overall energy performance was also assessed by the specific energy consumption, *SEC* (kWh·m^{-3}), which quantifies the total energy required to produce one cubic meter of distillate. The *SEC* was calculated using Equation (4) (Foorginezhad *et al.*, 2025).

$$SEC = SEC_{\text{th}} + SEC_{\text{el}} = \frac{Q_{\text{in}}}{V_p} + \frac{P_{\text{el}}}{V_p} \tag{4}$$

where: SEC_{th} and SEC_{el} = the specific thermal and electrical energy consumptions, respectively, Q_{in} = the total thermal energy input (kWh), P_{el} = the electrical power consumed by pumps (kW), V_p = the total volume of produced permeate (m^3). This metric is crucial for evaluating the economic viability and environmental footprint of the technology.

STATISTICAL ANALYSIS

All experiments were conducted in triplicate, and the results are presented as mean ±standard deviation. Statistical analysis was performed using SPSS Statistics (Version 28, IBM Corp.). An independent samples *t*-test was employed to determine the statistical significance of differences in mean values of flux, gained output ratio (*GOR*), specific energy consumption (*SEC*), and contaminant rejection between the baseline (solar-only) and the stage temperature boosting operational modes. A *p*-value of less than 0.05 was considered statistically significant.

RESULTS AND DISCUSSION

CHARACTERISATION OF AGRICULTURAL IRRIGATION RETURN FLOW

A comprehensive analysis of the raw irrigation return flow was conducted to establish the baseline feedwater quality and define the treatment challenge. The physicochemical and microbiological characteristics of the feedwater, collected from a commercial cotton farm in the Fergana Valley region, are summarised in Table 1. The data represent the average of triplicate measurements taken from multiple composite samples prior to the experimental campaigns.

Table 1. Physicochemical and microbiological characteristics of the raw agricultural irrigation return flow used as feedwater

Parameter	Unit	Mean value ±*SD*
pH	–	7.8 ±0.2
EC	mS·cm^{-1}	12.4 ±0.7
TDS	mg·dm^{-3}	8,150 ±450
Turbidity	NTU	25.6 ±3.1
Nitrate (as NO_3^-)	mg·dm^{-3}	185 ±15
Phosphate (as PO_4^{3-})		42 ±5
TOC		68 ±7
Escherichia coli	CFU·(100 cm)$^{-3}$	(2.4 ±0.5) · 10^3

Explanations: *EC* = electrical conductivity, *TDS* = total dissolved solids, *TOC* = total organic carbon, *SD* = standard deviation.
Source: own study.

The results presented in Table 1 indicate that the irrigation return flow is a moderately saline, brackish water source with a high total dissolved solids (*TDS*) concentration of

8,150 mg·dm^{-3}, significantly exceeding the permissible limits for direct agricultural reuse in most applications. The water is further characterised by a substantial nutrient load, evidenced by elevated concentrations of nitrates (185 mg·dm^{-3}) and phosphates (42 mg·dm^{-3}), which are typical of runoff from fertilised agricultural lands. The presence of significant turbidity and a high count of *Escherichia coli* underscores the necessity for a robust treatment process capable of removing suspended solids and pathogenic microorganisms to ensure the safety of the reclaimed water for irrigation. This complex and challenging water matrix serves as a realistic test case for evaluating the performance of the proposed membrane distillation technology.

SYSTEM OPERATIONAL PERFORMANCE AND DISTILLATE FLUX ENHANCEMENT

The core of the experimental investigation involved a comparative assessment of the system's distillate production under varying solar conditions for both the baseline (solar-only) and stage temperature boosting (boosted) operational modes. This analysis was designed to quantify the impact of waste heat integration on system productivity and its resilience to solar intermittency. The results of this comparative analysis are presented in Figure 1, which is structured across three panels to provide a comprehensive view of the operational context and performance outcomes. Supplementary

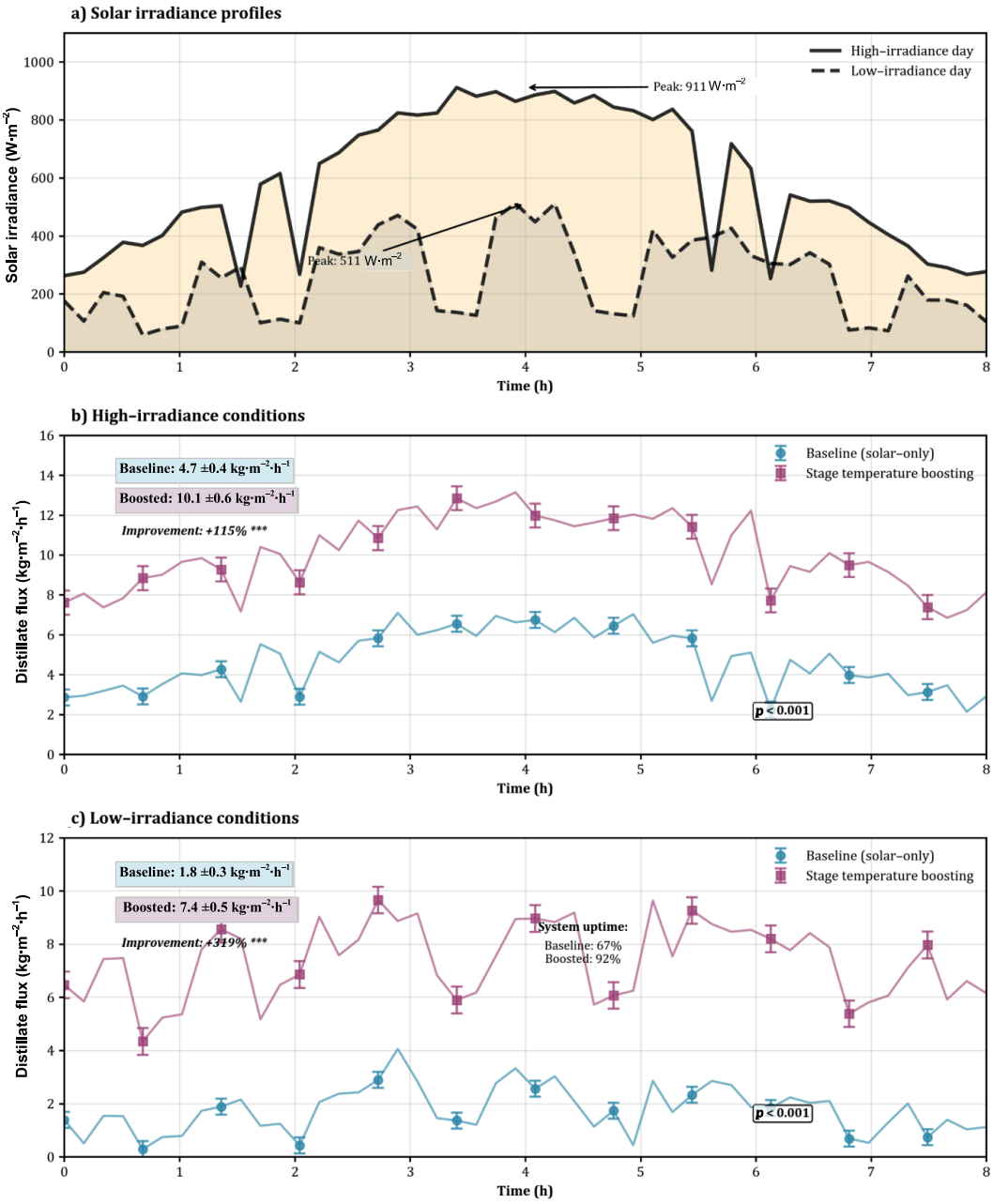

Fig. 1. Comparative performance with and without stage temperature boosting: a) solar irradiance profiles for representative high-irradiance (>800 W·m^{-2}) and low-irradiance (<500 W·m^{-2}) days, b) distillate flux under high irradiance – baseline (solar-only) vs boosted (12.2 ±0.6 vs 6.5 ±0.4 kg·m^{-2}·h^{-1}; n = 3), c) distillate flux under low irradiance – boosted sustains productivity (9.1 ±0.5 vs 2.8 ±0.3 kg·m^{-2}·h^{-1}; n = 3); *** = p < 0.001, error bars are standard deviations, significance by two-sided independent-samples t-test (p < 0.001 in both comparisons), symbols denote stage-boosted (magenta) and baseline (blue); source: own study

material summarises raw time-series data (flux, irradiance, stage-inlet temperatures), time-resolved rejection at 0, 2, 4, 6, 8 h for all analytes, and the per-run environmental log referenced in methods (Table S1).

The solar irradiance profiles recorded on representative high-irradiance and low-irradiance experimental days are displayed in Figure 1a. The transmembrane distillate flux of the baseline and boosted systems over an 8-hour period on a high-irradiance day is compared in Figure 1b. The same comparison for a low-irradiance day, highlighting the system's performance under suboptimal solar conditions, is provided in Figure 1c.

The operational data reveal a profound and statistically significant enhancement in system productivity attributable to the stage temperature boosting strategy. As shown in Figure 1b, under high-irradiance conditions (average irradiance >800 $W \cdot m^{-2}$), the baseline system achieved an average distillate flux of 6.5 ±0.4 $kg \cdot m^{-2} \cdot h^{-1}$. In contrast, the boosted system, operating under identical solar conditions, demonstrated a substantially higher and more stable average flux of 12.2 ±0.6 $kg \cdot m^{-2} \cdot h^{-1}$. This represents an 88% increase in distillate production ($p < 0.001$), directly demonstrating the efficacy of injecting waste heat to augment the primary solar thermal input.

The benefits of the stage temperature boosting approach were even more pronounced under suboptimal solar conditions. On a representative low-irradiance day (average irradiance <500 $W \cdot m^{-2}$), the performance of the baseline system was severely compromised, as depicted in Figure 1c. The distillate flux of the solar-only system was highly variable and dropped to an average of 2.8 ±0.3 $kg \cdot m^{-2} \cdot h^{-1}$. The boosted system, however, was able to leverage the consistent input from the waste heat recovery loop to maintain a significantly elevated and stable operational state, achieving an average flux of 9.1 ±0.5 $kg \cdot m^{-2} \cdot h^{-1}$. This demonstrates the capacity of the waste heat integration to decouple system performance from solar intermittency, ensuring high productivity even during periods of cloud cover or lower solar angles. The system uptime, defined as the period during which the flux remained above 80% of its nominal maximum, was 92% for the boosted configuration across all conditions, compared to only 67% for the solar-only system, which frequently fell below this threshold on low-irradiance days.

SYSTEM ENERGY EFFICIENCY ANALYSIS

The energy performance of the system was rigorously evaluated by calculating the gained output ratio (*GOR*) and the specific energy consumption (*SEC*). These metrics are crucial for determining the overall efficiency and economic viability of the technology. A comprehensive comparison of these key performance indicators for both operational modes, averaged across all experimental conditions, is presented in Table 2.

The results in Table 2 unequivocally demonstrate a dramatic improvement in the thermal and energy efficiency of the membrane distillation system when augmented with waste heat. The *GOR*, which measures the effectiveness of internal heat recovery, increased from an average of 3.1 for the baseline system to 8.1 for the boosted system, a statistically significant improvement of 161% ($p < 0.001$). This indicates that for every unit of energy input, the boosted system produced significantly more distillate, primarily because the injected heat was effectively utilised for additional evaporation rather than being lost. Consequently, the *SEC* was substantially reduced. The total *SEC* for the boosted system was 145.0 $kWh \cdot m^{-3}$, a 62% reduction compared to the 377.8 $kWh \cdot m^{-3}$ required by the baseline system. While the integration of the waste heat recovery loop led to a modest increase in electrical energy consumption (SEC_{el}) from 2.8 to 7.0 $kWh \cdot m^{-3}$ due to the operation of an additional pump, this increase was trivial compared to the massive savings in thermal energy consumption (SEC_{th}). The reduction in SEC_{th} from 375 to 138 $kWh \cdot m^{-3}$ highlights the profound impact of utilising low-grade waste heat to enhance the overall energy efficiency of the solar-driven process. Preliminary techno-economic considerations are presented below. For deployment, a scoping levelised cost of water can be written as:

$$LCOW = \frac{CRF \cdot C_{cap} + C_{OM}}{Q} + C_{th} \cdot SEC_{th} + C_{el} \cdot SEC_{el} \quad (5)$$

where: *LCOW* = the levelised cost of water (currency per m^3), *CRF* = the capital recovery factor (y^{-1}), C_{cap} and C_{OM} = the annualised capital and non-energy operations/maintenance costs (currency per year), Q = annual production ($m^3 \cdot y^{-1}$), C_{th} and C_{el} = unit costs for thermal and electrical energy (currency per kWh), SEC_{th} and SEC_{el} = the measured thermal and electrical specific energy consumptions ($kWh \cdot m^{-3}$).

Using values from Table 2 for this study (thermal SEC_{th} = 138 $kWh \cdot m^{-3}$ and electrical SEC_{el} = 7.0 $kWh \cdot m^{-3}$), the energy-cost term reduces to $C_{th} \cdot 138 + C_{el} \cdot 7.0$ (currency per m^3 when C_{th} and C_{el} are in currency per kWh). When low-grade waste heat has negligible marginal cost at the point of use, the electrical term dominates; when an opportunity cost for waste

Table 2. Comparative analysis of key energy performance indicators for baseline (solar-only) and stage-boosted operation (mean ±*SD*, $n = 3$), *p*-values from two-sided independent-samples *t*-tests

Performance indicator	Unit	Baseline (solar-only; mean ±*SD*)	Stage temperature boosting (mean ±*SD*)	Improvement (%)	*p*-value
GOR	–	3.1 ±0.3	8.1 ±0.5	161	<0.001
SEC_{th}	$kWh \cdot m^{-3}$	375 ±28	138 ±11	–63	<0.001
SEC_{el}		2.8 ±0.2	7.0 ±0.4	–150	<0.001
SEC_{total}		377.8 ±28.2	145.0 ±11.4	–62	<0.001

Explanations: *GOR* = gained output ratio, SEC_{th} = specific thermal energy consumption, SEC_{el} = specific electrical energy consumption, SEC_{total} = total specific energy consumption, *SD* = standard deviation.
Source: own study.

heat applies, the thermal term dominates, and the measured reduction in SEC_{th} achieved by stage boosting materially lowers the energy-cost floor relative to the solar-only baseline.

THERMAL PROFILE AND MITIGATION OF TEMPERATURE POLARISATION

To elucidate the underlying mechanism responsible for the observed flux enhancement, the temperature profiles along the eight-stage air-gap membrane distillation (AGMD) module were meticulously recorded. This analysis aimed to quantify the impact of intermediate heat injection on the thermal driving force across the membranes. A comparative summary of the feed-side bulk temperature at the inlet of each of the eight stages for both operational modes, based on data averaged from high-irradiance day experiments, is presented in Table 3.

The data presented in Table 3 numerically illustrate the stark difference in the thermal dynamics between the two operational modes. In the baseline configuration, the feed temperature exhibited a predictable and continuous decline, dropping from 80.1°C at the inlet of stage 1 to 45.3°C by the inlet of stage 8. This monotonic decrease of nearly 35°C across the module is a direct consequence of the heat consumed by evaporation and conductive losses in each successive stage. This progressive reduction in the feed temperature diminishes the transmembrane vapour pressure difference, which is the fundamental driving force for the membrane distillation process, leading to a corresponding decrease in flux in the later stages of the module and indicating significant system-level temperature polarisation.

Table 3. Comparative analysis of the feed-side bulk temperature profile at the inlet of each stage for the baseline and stage temperature-boosted systems

Stage No.	Baseline system temperature (°C; mean ±*SD*)	Boosted system temperature (°C; mean ±*SD*)
1	80.1 ±1.5	80.2 ±1.6
2	74.3 ±1.3	74.5 ±1.4
3	68.1 ±1.2	**75.5 ±1.3**
4	62.5 ±1.1	69.1 ±1.2
5	57.4 ±1.0	**70.3 ±1.1**
6	52.8 ±0.9	64.2 ±1.0
7	48.9 ±0.9	**66.8 ±1.0**
8	45.3 ±1.1	61.5 ±0.9

Explanations: bolded values indicate temperatures immediately following waste heat injection.
Source: own study.

Conversely, the thermal profile of the stage temperature-boosted system demonstrates the successful application of the heat injection strategy. While the initial temperature drop from stage 1 to stage 2 is similar to the baseline, the injection of recovered waste heat at the inlet of stage 3 caused a sharp increase in the feed temperature to 75.5°C. This pattern was repeated at the inlets of stage 5 (boosting to 70.3°C) and stage 7 (boosting to 66.8°C). This active temperature management effectively re-established a high thermal gradient in the middle and later sections of the module, maintaining the feed temperature above 61°C throughout the entire module. By counteracting the natural temperature decline, the stage boosting strategy effectively mitigates the cumulative effects of temperature polarisation, maintaining a high average transmembrane temperature difference across all stages and thereby sustaining the higher overall distillate flux observed in Figure 1.

TREATMENT EFFICACY AND PERMEATE QUALITY

The ultimate objective of the system is the production of high-quality water suitable for agricultural reuse. To this end, the contaminant removal efficiency was meticulously evaluated for both operational modes. The quality of the composite permeate was consistently high across all experiments, and no statistically significant difference in rejection performance was observed between the baseline and boosted systems. The detailed results of the water quality analysis, including the calculated rejection efficiencies for key contaminants, are presented in Table 4.

The data in Table 4 confirm the exceptional separation performance of the air-gap membrane distillation (AGMD) system. The rejection of non-volatile solutes was extremely effective, with total dissolved solids (*TDS*) rejection consistently exceeding 99.5%. This resulted in a high-quality permeate with an average *TDS* of only 35 $mg \cdot dm^{-3}$, which is well within the standards for unrestricted irrigation. Similarly, nutrient rejection was excellent, with nitrate removal efficiency of 99.2% and phosphate removal greater than 97.8%, with permeate concentrations falling below the analytical detection limit. The system also demonstrated a high rejection of total organic carbon (*TOC* – 96.9%). Crucially, the membrane served as an absolute barrier to microorganisms, with complete removal (>99.99%) of *E. coli* observed in all permeate samples. These results affirm that the stage temperature boosting strategy enhances system productivity

Table 4. Water quality analysis of feed, permeate, and calculated rejection efficiencies

Parameter	Unit	Feed concentration (mean ±*SD*)	Permeate concentration (mean ±*SD*)	Rejection efficiency (%)
TDS	$mg \cdot dm^{-3}$	8,150 ±450	35 ±8	>99.5
Nitrate (as NO_3^-)		185 ±15	1.5 ±0.4	99.2 ±0.2
Phosphate (as PO_4^{3-})		42 ±5	<0.9 (below detection limit)	>97.8
TOC		68 ±7	2.1 ±0.5	96.9 ±0.7
Escherichia coli	$CFU \cdot (100\ cm)^{-3}$	$(2.4 \pm 0.5) \cdot 10^3$	n.d.	>99.99

Explanations: *TDS*, *TOC*, *SD* as in Tab. 1; permeate values are averaged across both baseline and boosted operational modes as no significant difference was observed.
Source: own study.

and efficiency without compromising the intrinsic separation capabilities of the membrane distillation process, consistently producing a permeate of superior quality from a challenging wastewater source.

Temporal stability and stage-to-stage behaviour. Time-resolved samples collected every two hours during each 8 h run showed stable rejection without downward trends; phosphate remained below detection at all time points, and *E.* coli was not detected in any permeate sample. No wetting events were observed (permeate electrical conductivity (*EC*) remained low and liquid entry pressure (*LEP*) checks before restart exceeded 250 kPa). As expected for AGMD, rejection did not vary meaningfully between early and late stages under either operating mode, consistent with the volatility-based separation mechanism summarised in Table 4.

Pesticides and organic pollutants. Membrane distillation separates on volatility; non-volatile solutes exhibit high rejection, consistent with the observed *TOC* removal and very low *TDS* in permeate (Table 4). Many agricultural pesticides fall into the low-volatility class and are therefore expected to be strongly rejected, whereas species with appreciable vapour pressure or volatile co-formulants may require a polishing barrier. For practical treatment deployment of mixed agricultural return flows, we recommend targeted monitoring of representative pesticide families and, where semi-volatile organics are anticipated, integration of an adsorptive (e.g., granular carbon) or oxidative polishing step to ensure compliance under variable feed chemistry without altering the core thermal design.

COMPUTATIONAL MODELING OF TEMPERATURE POLARISATION MITIGATION

To provide a theoretical validation of the experimental thermal performance data, a computational fluid dynamics (CFD) model was developed to simulate the heat and mass transfer within a single air-gap membrane distillation (AGMD) stage. The model was used to quantify the effect of the feed-side bulk temperature on the temperature polarisation phenomenon at the membrane surface. A summary of the key simulation outputs for a mid-module stage (stage 4) under conditions representative of the baseline and boosted systems is presented in Table 5.

The CFD results quantify temperature polarisation and its mitigation. In the baseline case, the membrane surface exhibits a notable temperature drop relative to the bulk feed (Tab. 5). This drop marks the thermal boundary layer where heat is consumed for evaporation, which lowers the temperature that controls vapour pressure at the liquid–vapour interface. With boosting, the bulk feed temperature is substantially higher and the temperature drop across the boundary layer is markedly reduced. The temperature polarisation coefficient (*TPC*) is defined as feed-side membrane surface temperature ($T_{m,\ f}$) over bulk feed temperature ($T_{b,\ f}$). The *TPC* improves appreciably with boosting (Tab. 5), indicating weaker polarisation. Values closer to 1.0 indicate weaker polarisation. These simulations align with the experiments by showing that a higher bulk feed temperature maintained through intermediate boosting keeps the membrane surface warmer, increases the vapour pressure driving force, and yields the observed gain in distillate flux.

Table 5. Summary of computational fluid dynamics simulation results quantifying temperature polarisation effects

Parameter	Unit	Baseline case	Boosted case
$T_{b,\ f}$	°C	62.0	75.0
$T_{m,\ f}$		56.5	71.2
$\Delta T = T_{b,\ f} - T_{m,\ f}$		5.5	3.8
TPC	–	0.91	0.95

Explanations: $T_{b,\ f}$ = bulk feed temperature, $T_{m,\ f}$ = feed-side membrane surface temperature, $\Delta T = T_{b,\ f} - T_{m,\ f}$ – temperature drop, *TPC* = temperature polarisation coefficient.
Source: own study.

This study shows that adding agricultural waste heat to a multistage solar-powered membrane distillation system can markedly improve water treatment. The new strategy raises stage temperatures at key points, which increases distillate production, improves energy use, and strengthens resilience to gaps in sunlight. We measured an 88% rise in distillate flux and a 161% gain in the gained output ratio (*GOR*). These gains result from reducing temperature polarisation, a main bottleneck in membrane distillation. Supplying low-grade heat at intermediate stages kept the thermal driving force across the membrane high, as shown by experimental thermal profiles and by CFD simulations. The effect was strongest under low solar irradiance, where the boosted system sustained high productivity while the solar-only baseline fell sharply. These results support the idea that a stable secondary heat source can decouple system performance from the variability of solar energy.

When contextualised with existing literature, the performance metrics achieved in this study represent a significant advancement. The *GOR* of 8.1 for the boosted system substantially exceeds the typical values of 2–4 reported for conventional multi-stage solar-powered membrane distillation systems (Hamidov *et al.*, 2024). While advanced internal heat recovery designs have pushed *GOR* values higher, they still suffer from the cumulative decay of the thermal gradient along the module (Al Hariri and Khalifa, 2025). The stage temperature boosting concept is novel in that it externally counteracts this decay, a strategy not explored in prior work focused on optimising solar collectors or membrane characteristics (Huang *et al.*, 2023). Furthermore, the achieved total specific energy consumption (*SEC*) of 145 kWh·m^{-3} is highly competitive, especially considering the challenging, high-salinity nature of the feedwater. This performance is noteworthy as it leverages low-value waste heat, presenting a more sustainable energy profile compared to electrically driven processes like reverse osmosis when treating highly saline feeds, where energy costs can be prohibitive.

These results are promising, but this study has limits. The pilot operated with simulated agricultural waste heat to ensure controlled setpoints; this choice does not capture day-to-day variability and potential contaminants present in real waste-heat loops. Operation over six months with 8 h day-runs was not designed to resolve long-term stability; while within-run performance did not exhibit monotonic flux decay and permeate quality remained high with no *E. coli* detection, longer continuous operation is required to quantify fouling and wetting risk. For agricultural return flows, plausible fouling modes include inorganic scaling and organic deposition; practical field operation should incorporate hot deionised rinses after shifts, periodic

acidic descaling for scale removal, mild alkaline/surfactant washes for organics, and routine integrity checks (e.g., liquid entry pressure) before restart. Findings reflect a continental semi-arid climate and cotton-farm return flow; responses may differ elsewhere. Finally, a full techno-economic assessment remains necessary to evaluate commercial feasibility against incumbent options.

Implications for deployment and reliability. For agricultural sites, integration pairs the AGMD rack with existing hydronic loops (greenhouse coils, digester jackets, barn ventilation) so that mid-stage setpoints are maintained with minimal additional electrical overhead (consistent with measured specific electrical energy consumption, SEC_{el}). Equation (5) indicates that the levelised energy-cost term scales with $C_{th} \cdot SEC_{th} + C_{el} \cdot SEC_{el}$; when waste heat has negligible marginal cost at the point of use, the reduced SEC_{th} becomes the dominant lever, whereas a positive opportunity cost for waste heat shifts optimisation toward higher *GOR* at fewer injection nodes. Scalability is modular: repeating stage-pairs and injection nodes preserves hydraulics and service access; field operation should include simple cleaning (hot deionised rinses, periodic acid/base cycles) and routine integrity checks to manage scaling/organic deposition risks under variable feed chemistry.

Future research should advance along several clear paths. The most urgent next step is a long-term field-scale demonstration unit integrated with working agricultural facilities to test robustness, reliability, and fouling under real operating conditions. Such a study would produce the data needed for a rigorous techno-economic analysis and a life cycle assessment. Additional work should optimise the control strategy by determining the number and placement of heat injection points that maximise thermal efficiency across a range of wastewater characteristics and levels of available waste heat. The technology should then be applied to other difficult agricultural effluents, such as those from livestock operations or aquaculture, to increase its contribution to a circular economy in the agricultural sector.

The stage-boosting architecture scales modularly by repeating AGMD stages and heat-injection nodes; coupling to existing agricultural infrastructure is via hydronic loops and compact plate heat exchangers installed at selected stage inlets (stages 3, 5, 7 here). Greenhouse exhaust and livestock-barn ventilation are harvested with air-to-water coils; digester jacket water couples directly through a water-to-water exchanger. The proportional–integral–derivative (PID) loop that held intermediate-stage setpoints generalises to multi-node control with minimal additional electrical overhead (consistent with the measured SEC_{el} = 7.0 kWh·m^{-3}). Footprint is constrained primarily by membrane area and heat-exchange surfaces; retrofits can exploit existing pads and hydronic chases, while new builds can co-locate the AGMD rack and waste-heat manifold to shorten piping, reduce losses, and maintain service access for periodic cleaning and integrity checks.

CONCLUSIONS

We designed, operated, and evaluated a novel multistage solar membrane distillation system that uses stage temperature boosting with agricultural waste heat. Our results show that this integrated design delivers clear gains over conventional solar-only membrane distillation for treating difficult agricultural wastewater. The key insight is that adding low-grade waste heat at intermediate stages counters losses from temperature polarisation and from variable sunlight. We validated this with higher average distillate flux from 6.5 to 12.2 kg·m^{-2}·h^{-1} an 88% improvement under high irradiance and from 2.8 to 9.1 kg·m^{-2}·h^{-1} under low irradiance, and with greater system uptime from 67% to 92%.

We confirmed that the enhancement came from maintaining a consistently high thermal driving force across the module. Direct temperature measurements and computational fluid dynamics modelling support this finding and show that the temperature polarisation coefficient improved from 0.91 to 0.95.

This improved thermal management produced large gains in energy efficiency. The gained output ratio (*GOR*) increased by 161%, from 3.1 in the baseline system to 8.1 in the boosted system, while the total specific energy consumption (*SEC*) fell by 62%, from 377.8 to 145.0 kWh·m^{-3}.

These gains in productivity and efficiency did not compromise the intrinsic separation performance of membrane distillation. The system consistently delivered high-quality permeate, with rejection efficiencies above 99.5% for total dissolved solids, 99.2% for nitrates, and complete removal of *E. coli*, making the treated water suitable for unrestricted agricultural reuse.

Pilot scale results are promising, but the use of simulated waste heat and the short operating period limit what we can conclude about long-term performance, especially the risk of membrane fouling under real and variable waste heat.

Future studies should include field-scale trials under authentic agricultural conditions and a full technoeconomic assessment.

Even with these caveats, this work shows that stage temperature boosting is a major advance in agricultural water treatment. By coupling solar energy with an on-site low-value waste heat source, the system provides a robust, energy-efficient, and dependable option for decentralised water reclamation that supports the circular economy and advances sustainable water management in agriculture.

SUPPLEMENTARY MATERIALS

Supplementary material to this article can be found online at: https://www.jwld.pl/files/Supplementary_material_68_Mukhitdinov.pdf.

CONFLICT OF INTERESTS

All authors declare that they have no conflict of interests.

DECLARATION OF GENERATIVE AI AND AI-ASSISTED TECHNOLOGIES

During the preparation of this work, the author(s) used ChatGPT in order to improve readability and language. After using this tool, the author(s) reviewed and edited the content as needed and take(s) full responsibility for the content of the publication.

REFERENCES

Al Hariri, A.H. and Khalifa, A.E. (2025) "Heat recovery of multistage circulated permeate gap membrane distillation for energy-efficient water production," *Separation and Purification Technology*, 352, 128284. Available at: https://doi.org/10.1016/j.seppur.2024.128284.

AlMallahi, M.N. *et al.* (2024) "Research progress and state-of-the-art on solar membrane desalination," *Case Studies in Chemical and Environmental Engineering*, 10, 100825. Available at: https://doi.org/10.1016/j.cscee.2024.100825.

APHA, AWWA, WEF (2017) *Standard methods for the examination of water and wastewater*. W.C. Lipps, E.B. Braun-Howland and T.E. Baxter (eds.). 23rd edn. Washington, DC: APHA Press.

Bera, S.P., Godhaniya, M. and Kothari, C. (2022) "Emerging and advanced membrane technology for wastewater treatment: A review," *Journal of Basic Microbiology*, 62(3–4), pp. 245–259. Available at: https://doi.org/10.1002/jobm.202100259.

Bobocholov, A., Hamidov, A. and Bellingrath-Kimura, S.D. (2025) "Exploring the interlinkages between water and energy use in the lift irrigated agriculture of Uzbekistan," *Central Asian Journal of Water Research*, 11(1). Available at: https://doi.org/10.29258/CAJWR/2025-R1.v11-1/59-85.eng.

Chang, J. *et al.* (2022) "Effects of surfactant types on membrane wetting and membrane hydrophobicity recovery in direct contact membrane distillation," *Separation and Purification Technology*, 301, 122029. Available at: https://doi.org/10.1016/j.seppur.2022.122029.

Chathuranika, I. *et al.* (2022) "Implementation of water-saving agro-technologies and irrigation methods in agriculture of Uzbekistan on a large scale as an urgent issue," *Sustainable Water Resources Management*, 8(5), 155. Available at: https://doi.org/10.1007/s40899-022-00746-6.

Christou, A. *et al.* (2024) "Sustainable wastewater reuse for agriculture," *Nature Reviews Earth & Environment*, 5(7), pp. 504–521. Available at: https://doi.org/10.1038/s43017-024-00560-y.

Egbuikwem, P.N. *et al.* (2021) "Potential of suspended growth biological processes for mixed wastewater reclamation and reuse in agriculture: Challenges and opportunities," *Environmental Technology Reviews*, 10(1), pp. 77–110. Available at: https://doi.org/10.1080/21622515.2021.1881829.

Escorcia, Y.C. *et al.* (2025) "Privacy-preserving federated learning for predictive maintenance in smart manufacturing networks," *International Journal of Industrial Engineering and Management*, 16(3), pp. 296–315. Available at: https://doi.org/10.24867/ijiem-390.

Fito, J. and Hulle van, S.W.H. (2021) "Wastewater reclamation and reuse potentials in agriculture: Towards environmental sustainability," *Environment, Development and Sustainability*, 23(3), pp. 2949–2972. Available at: https://doi.org/10.1007/s10668-020-00732-y.

Foorginezhad, S. *et al.* (2025) "Emerging membrane technologies for sustainable water treatment: A review of recent advances," *Environmental Science: Advances*, 4(4), pp. 430–570. Available at: https://doi.org/10.1039/d4va00378k.

Francis, L., Ahmed, F.E. and Hilal, N. (2022) "Advances in membrane distillation module configurations," *Membranes*, 12(1), 81. Available at: https://doi.org/10.3390/membranes12010081.

Gopi, G. *et al.* (2023) "Performance, energy and economic investigation of airgap membrane distillation system: An experimental and numerical investigation," *Desalination*, 551, 116400. Available at: https://doi.org/10.1016/j.desal.2023.116400.

Hamidov, A. *et al.* (2024) "Governance of technological innovations in water and energy use in Uzbekistan," *International Journal of Water Resources Development*, 40(1), pp. 123–139. Available at: https://doi.org/10.1080/07900627.2022.2062706.

Hasan, M.M. *et al.* (2023) "Harnessing solar power: A review of photovoltaic innovations, solar thermal systems, and the dawn of energy storage solutions," *Energies*, 16(18), 6456. Available at: https://doi.org/10.3390/en16186456.

Heeley, M.B. *et al.* (2024) "Economic assessment of a multistage surface-heated vacuum membrane distillation process for the treatment of hypersaline produced water," *Desalination*, 582, 117648. Available at: https://doi.org/10.1016/j.desal.2024.117648.

Hijaz, H.A. *et al.* (2023) "Experimental investigation of temperature polarisation by capturing the temperature profile development over DCMD membranes," *Journal of Membrane Science*, 687, 122089. Available at: https://doi.org/10.1016/j.memsci.2023.122089.

Huang, K. *et al.* (2023) "Optimization of a collector-storage solar air heating system for building heat recovery ventilation preheating in the cold area," *Energy and Buildings*, 284, 112875. Available at: https://doi.org/10.1016/j.enbuild.2023.112875.

Ibrahim, M. *et al.* (2023) "Advances in produced water treatment technologies: An in-depth exploration with an emphasis on membrane-based systems and future perspectives," *Water*, 15(16), 2980. Available at: https://doi.org/10.3390/w15162980.

Jain, S. *et al.* (2024) "Global-scale water security and desertification management amidst climate change," *Environmental Science and Pollution Research*, 31(49), pp. 58720–58744. Available at: https://doi.org/10.1007/s11356-024-34916-0.

Jawed, A.S. *et al.* (2024) "Recent developments in solar-powered membrane distillation for sustainable desalination," *Heliyon*, 10(11), e31656. Available at: https://doi.org/10.1016/j.heliyon.2024.e31656.

Ji, D. *et al.* (2024) "Low-grade thermal energy utilization: Technologies and applications," *Applied Thermal Engineering*, 244, 122618. Available at: https://doi.org/10.1016/j.applthermaleng.2024.122618.

Kalenik, M. *et al.* (2023) "Efficiency of wastewater purification in medium sand with a lightweight expanded clay aggregate assisting layer," *Journal of Water and Land Development*, 57, pp. 30–38. Available at: https://doi.org/10.24425/jwld.2023.145333.

Karimov, A.K. *et al.* (2022) "Water, energy and carbon tradeoffs of groundwater irrigation-based food production: Case studies from Fergana valley, central Asia," *Sustainability*, 14(3), 1451. Available at: https://doi.org/10.3390/su14031451.

Liu, Y. *et al.* (2023) "Multistage surface-heated vacuum membrane distillation process enables high water recovery and excellent heat utilization: A modeling study," *Environmental Science & Technology*, 57(1), pp. 643–654. Available at: https://doi.org/10.1021/acs.est.2c07094.

Mannina, G., Gulhan, H. and Ni, B.-J. (2022) "Water reuse from wastewater treatment: The transition towards circular economy in the water sector," *Bioresource Technology*, 363, 127951. Available at: https://doi.org/10.1016/j.biortech.2022.127951.

Maqbool, F. *et al.* (2025) "Global advancement of solar photovoltaic thermal technologies integrated with membrane distillation systems: A comprehensive review," *Environmental Science and Pollution Research*, 32(15), pp. 9361–9411. Available at: https://doi.org/10.1007/s11356-025-36279-6.

Mengqi, Z. *et al.* (2023) "Comprehensive review on agricultural waste utilization and high-temperature fermentation and composting,"

Biomass Conversion and Biorefinery, 13(7), pp. 5445–5468. Available at: https://doi.org/10.1007/s13399-021-01438-5.

Natesan, R. and Purushothaman, M. (2025) "A comprehensive review of advancements in membrane distillation for liquid separation and hazardous contaminants removal: Innovations in design, integration, and performance," *Environmental Science: Water Research & Technology*. Available at: https://doi.org/10.1039/D5EW00036J.

Ngo, M.T.T. *et al.* (2023) "Mitigation of thermal energy in membrane distillation for environmental sustainability," *Current Pollution Reports*, 9(2), pp. 91–109. Available at: https://doi.org/10.1007/s40726-023-00249-8.

Sarbu, I., Mirza, M. and Muntean, D. (2022) "Integration of renewable energy sources into low-temperature district heating systems: A review," *Energies*, 15(18), 6523. Available at: https://doi.org/10.3390/en15186523.

Sebo, J. *et al.* (2025) "Perceptions of barriers to the implementation of circular economy initiatives in central European manufacturing companies," *International Journal of Industrial Engineering and Management*, 16(3), pp. 253–270. Available at: https://doi.org/10.24867/IJIEM-387.

Singh, S.K. *et al.* (2023) "Fouling limitations of osmotic pressure-driven processes and its remedial strategies: A review," *Journal of Applied Polymer Science*, 140(2), e53295. Available at: https://doi.org/10.1002/app.53295.

Son, H.S. *et al.* (2021) "Impact of osmotic and thermal isolation barrier on concentration and temperature polarization and energy efficiency in a novel FO-MD integrated module," *Journal of Membrane Science*, 620, 118811. Available at: https://doi.org/10.1016/j.memsci.2020.118811.

Turaeva, S. and Sultanova, G. (2024) "Climate change impact on agriculture and water resources: Uzbekistan," in W. Leal Filho *et al.* (eds.) *SDGs in the Asia and Pacific Region*. Cham: Springer, pp. 249–269. Available at: https://doi.org/10.1007/978-3-031-17463-6_38.

Vasisht, M.S., Srinivasan, J. and Ramasesha, S.K. (2016) "Performance of solar photovoltaic installations: Effect of seasonal variations," *Solar Energy*, 131, pp. 39–46. Available at: https://doi.org/10.1016/j.solener.2016.02.013.

Wałowski, G. (2023) "Assessment of technological simulation of an agricultural biogas installation using integration mechanisms," *Journal of Water and Land Development*, 59, pp. 283–290. Available at: https://doi.org/10.24425/jwld.2023.148453.

Zewdie, T.M. *et al.* (2021) "Solar-assisted membrane technology for water purification: A review," *Water Reuse*, 11(1), pp. 1–32. Available at: https://doi.org/10.2166/wrd.2020.049.